Geol. Mag. **145** (*5*), *2008, pp. 733–744. © 2008 Cambridge University Press*
doi:10.1017/S0016756808004974 *Printed in the United Kingdom*

Correlation of plume morphologies on joint surfaces with their fracture mechanic implications

D. BAHAT*‡, A. RABINOVITCH† & V. FRID*

*Department of Geological and Environmental Sciences Ben Gurion University of the Negev, POB 653 Beer Sheva, 84105 Israel, and the Deichmann Rock Mechanics Laboratory of the Negev
†Department of Physics, Ben Gurion University of the Negev, POB 653 Beer Sheva, 84105 Israel, and the Deichmann Rock Mechanics Laboratory of the Negev

(*Received* 14 May 2007; *accepted* 13 September 2007; First published online 13 June 2008)

Abstract – The fractography and conditions of propagation of joints that cut Devonian siltstones in the Appalachian Plateau, New York, and Eocene chalks from the Beer Sheva Syncline, Israel, are investigated. The joints cutting the siltstones are marked by S-type and C-type plumes, and the joints cutting the Lower Eocene and Middle Eocene chalks are marked by coarse and delicate plumes, respectively. The four plume types propagated under sub-critical (slow propagation) conditions. On the semi-quantitative fracture velocity (v) versus the tensile stress intensity (K_I) curves, the S and C plume types fall in the $K_I = 0.073$–0.79 MPa $m^{1/2}$ and $v = 2 \times 10^{-4}$–10^{-2} m/s and $K_I = 0.073$–0.79 MPa $m^{1/2}$ and $v = 10^{-6}$–10^{-4} m/s ranges respectively. The coarse and delicate plumes fall in the $K_I = 0.03$–0.17 MPa $m^{1/2}$ and $v = 10^{-6}$–4×10^{-5} m/s and $K_I = 0.03$–0.17 MPa $m^{1/2}$ and $v = 10^{-4}$–5×10^{-3} m/s ranges, respectively. Generally, slow plumes are relatively short, show periodicity, and typically exhibit superposition of arrest marks. On the other hand, faster plumes are longer and continuous, occur particularly in thinner layers, and show no superposition of arrest marks. There is a clear distinction between two en échelon segmentation end-members in the joint fringe, the 'discontinuous breakdown type' and the 'continuous breakdown type'. There are also 'transitional' variations between the end-members. Only curved 'discontinuous breakdown type' boundaries of en échelon fringes can be equated with mirror boundaries.

Keywords: jointing, plumes, fracture mechanics, boundaries.

1. Introduction

1.a. Fractography and fracture mechanics in rocks

Plumes represent one of the more important fractographic features commonly occurring on geological tensile fractures. This is useful for studying tectonophysics because the key fracture mechanic parameters, like the tensile stress intensity factor K_I (the product of multiplying the fracture stress by the square root of the fracture length) and the palaeostress magnitude, may be obtained from the fractographic features revealed on joint surfaces (Bahat, 1979). Plumes commonly start as straight striae, and their barbs splay towards the two rock boundaries (Fig. 1a). Bahat & Engelder (1984) investigated the fractographies of two joint sets in the Devonian siltstones from the Appalachian Plateau in New York, and distinguished between straight and continuous plumes (maintaining approximately the same morphology throughout its length) of the S-type (Fig. 1a), and the C-type plumes that were neither straight nor continuous. They were either curved and split into various directions (Fig. 1c), or showed rhythmic increase and decrease of plume intensities, that is, enlargement and diminution of depth and widths of the barbs (Fig. 1b). Transitional patterns between the curved and rhythmic (cyclic) styles were also common. Bahat & Engelder (1984) identified in the rhythmic C-type plumes the alternate short and long episodes of cracking, predicted by Secor (1965), suggesting slow fracturing. The latter fracturing was specified to be between the lower ranges of regions I and II of the velocity–stress intensity curve (Fig. 2).

Lacazette & Engelder (1992) diverged from the interpretations of Bahat & Engelder (1984) and suggested that the cyclic pattern of the rhythmic C-type plume (Fig. 1c) may arise from dynamic instability of the fracture–fluid–rock system, when $K_I > K_{Ic}$ (where K_{Ic} is the critical stress intensity). Hull (1999, p. 123) describes the increase in roughness beyond the mirror boundary, from the mirror plane, through the mist to the hackle zone, which is associated with increases in crack velocities and stress intensities under unstable conditions. Engelder (2004) suggests that surface roughness varies in the same manner during stable joint propagation, that is, below K_{Ic}. These and additional fractographic descriptions in New York and in other fracture provinces (e.g. Kulander, Barton & Dean, 1979; Simón, Arlegui & Pocoví, 2006) show how difficult the interpretation of joint fractography may be.

1.b. The mirror boundary

The fracture mechanic boundary between the sub-critical and post-critical regimes is set at K_{Ic} (Fig. 2). For a full understanding of the tectonic implications that might be derived by the interpretation of joint

‡Author for correspondence: bahat@bgu.ac.il

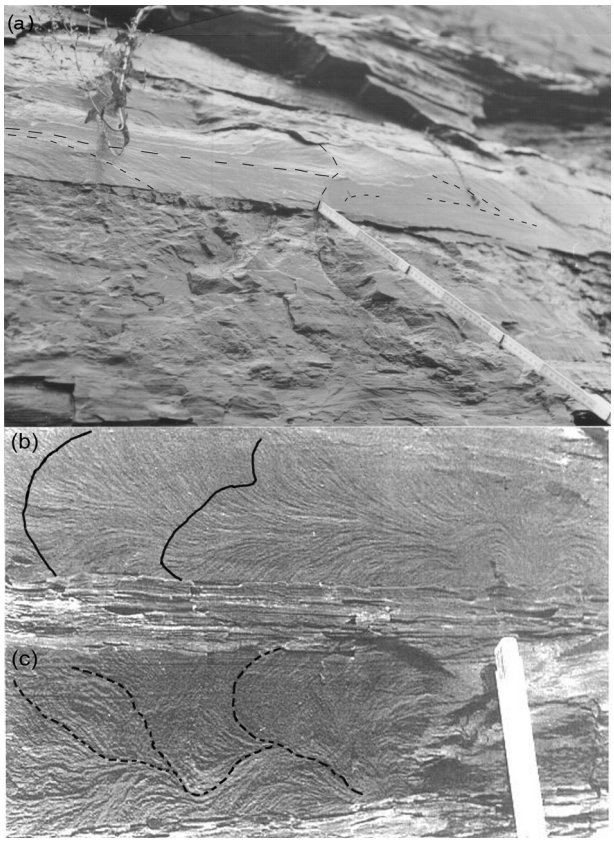

Figure 1. Three plume types propagating from right to left, in the Appalachian Plateau (modified from Bahat & Engelder, 1984). (a) Two joints decorated by 'straight' plumes meet at a junction (above scale) on a siltstone bed, 21 cm thick, intercalated in shales; both joints are oriented 345°. (b) 'Rhythmic' plume displays periodic fan perimeters (solid black lines), designating the fracture fronts where reduced fracture velocities occurred. (c) 'Curving' plume shows spreading of barbs to all directions (dashed black lines); both plumes mark joints oriented 335°, cutting adjacent siltstone beds (thickness of lower bed is 18 cm).

fracture surface morphology, there is a fundamental need to distinguish fractographically between these two regimes and identify their particular diagnostic features within the mirror plane and beyond it, respectively. The early history of the joint is recorded on the mirror plane, while the late one is marked on the fringe. Thus, a key criterion in characterizing the mirror plane is identifying the mirror boundary that separates the mirror plane and the fringe. In plutonic rocks, there are occasionally favourite conditions for finding clear boundaries between the mirror and hackle fringes. A definition of the mirror boundary in granite enabled the calculation of the palaeostresses that induced jointing in the rock (Bahat & Rabinovitch, 1988). Such clear boundaries also allowed the construction of a semi-quantitative fractographic curve of the fracture velocity (v) versus K_I for the analysis of granite fracture conditions during its cooling (Bahat, Bankwitz & Bankwitz, 2003). However, the identification of mirror boundaries on joints cutting sedimentary rocks is a more difficult task, as explained below.

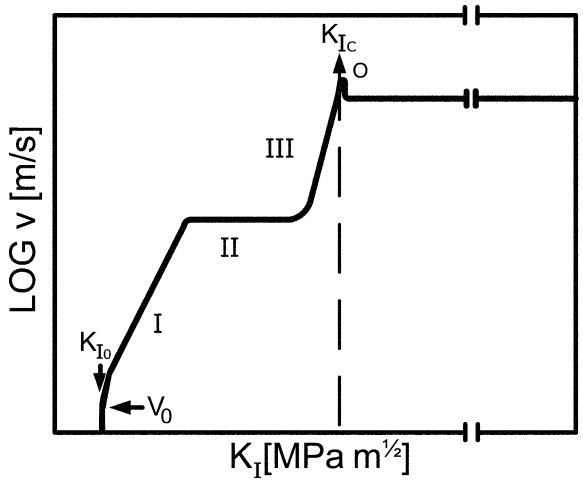

Figure 2. Schematic variation of stress intensity factor K with crack velocity V. The sub-critical curve left of K_{Ic} is divided into three regions I, II and III. K_0 and V_0 are the stress corrosion limit and the crack velocity at this limit (Wiederhorn & Bolz, 1970). Supercritical growth occurs mostly along a terminal velocity plateau following a rapid increase in crack velocity at K_{Ic} (modified from Evans, 1974). A velocity overshoot 'o' immediately after K_{Ic} before the plateau has been predicted by Rabinovitz & Bahat (1979).

1.c. Objectives of the present study

We set three objectives for the present investigation:

(1) To study three aspects of fracture mechanics that are connected to the formation of joints, starting with the elaboration on the boundaries of mirror planes, which are important in the interpretation of joint fractography.
(2) To extend the studies of the v versus K_I curve in relation to fractography from granites to sedimentary rocks, and construct four new semi-quantitative curves of the v versus K_I, correlative to plume morphology for two rock types. This would enable evaluation of the conditions of propagation of several joint sets from different localities, aiming at setting the stage for semi-quantitative analyses of their sub-critical jointing conditions.
(3) To demonstrate that the treatment of the fracture mechanics of jointing in sedimentary rocks must be carried out in close conjunction with the variability of the geological parameters.

2. Basic fractographic features on joint surfaces, with a special reference to the mirror plane boundary in sedimentary rocks

2.a. Geometric variations in the context of defining the mirror boundaries

There is a clear distinction between two en échelon segmentation types (Bahat, 1997): the 'discontinuous breakdown type', and the 'continuous breakdown type'. In the 'discontinuous breakdown type', the breakdown is 'discontinuous' along clear boundaries of the parent joints (Fig. 3a), while in the 'continuous breakdown

https://doi.org/10.1017/S0016756808004974 Published online by Cambridge University Press

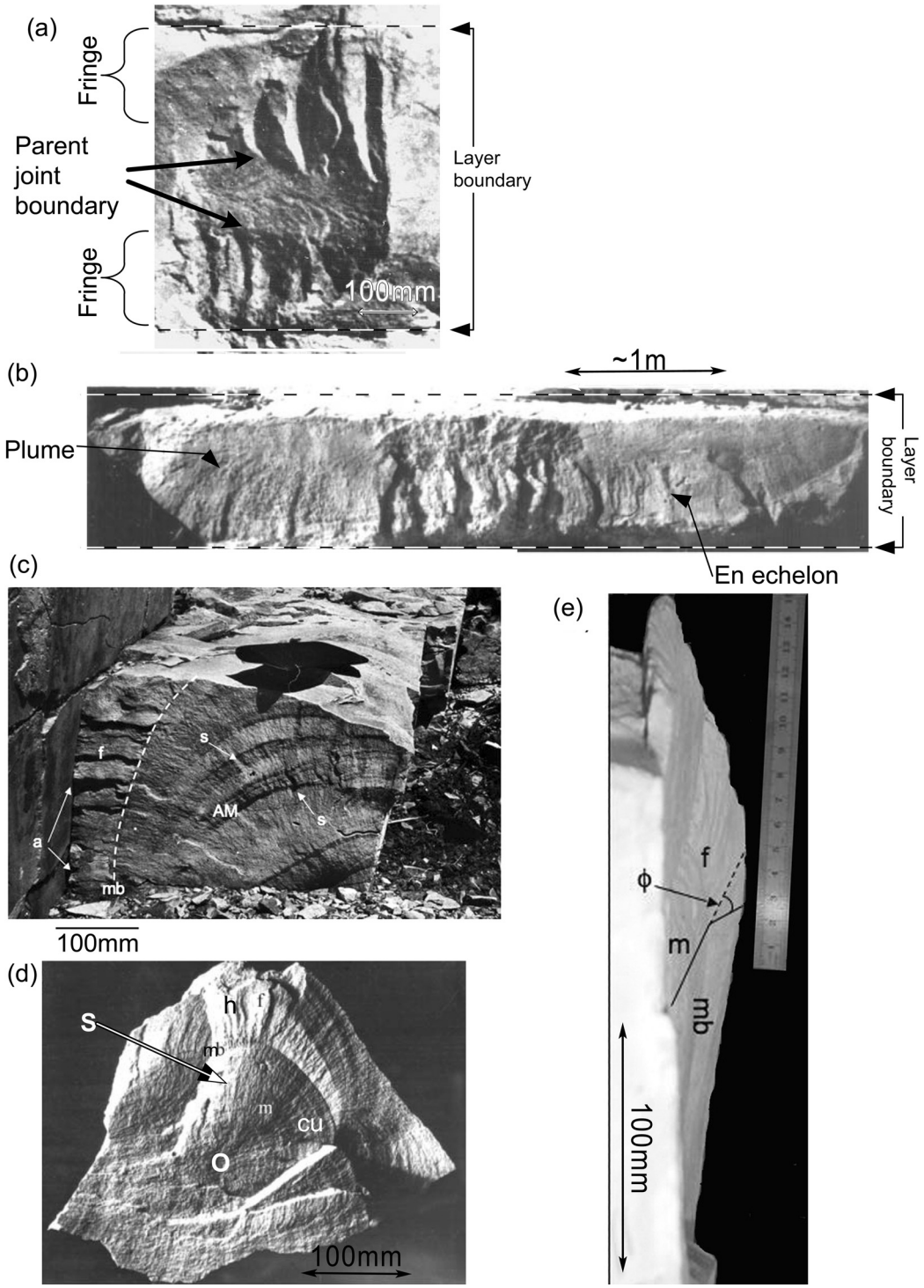

Figure 3. Different styles of boundaries separating the parent joints and fringes. (a) A joint cutting Lower Eocene chalk in the Shephela syncline. A 30 cm long plume propagates from left to right in the horizontal, rectangular parent joint. En échelon segments break down discontinuously, in the upper and lower fringes that occur between the parent joint boundaries and the layer boundaries (dashed lines), along which the rock is partly eroded (modified from Bahat, 1997). (b) A joint cutting Middle Eocene chalk, showing a delicate bilateral plume (barely visible) and a continuous breakdown of en échelon segmentation that starts from the centre of the parent joint, where segments propagate downward toward the lower layer boundary. Note en échelon growth in continuation of the plume (at left). Scale bar is 50 cm (modified from Bahat, 1987). (c) A joint from an orthogonal system, cutting chalk near Nazareth, Lower Galil, and arrests at a previous joint at left along a contact 'a'. A series of coarse, concentric arrest marks that have sharp crests indicate that the joint propagated from its lower right (the origin is hidden under ground) towards its upper left side. The joint surface is also decorated by delicate, radial striae, which become much more intense on cutting the arrest mark crests (at 's' locations). A curved mirror boundary, 'mb', separates between the mirror plane at right and the fringe, 'f', which is populated by a set of en échelon segments, at left. Note in addition: (1) slight splits of striae to plumes, at some locations (e.g. below the letters AM), and (2) the width of the fringe is determined by the geometric relationship of the orthogonal existing joint at 'a', setting a free surface, and the curved mirror boundary. (d) A joint cutting chalk, showing on the mirror plane, 'm', the location of fracture origin, 'o', concentric, delicate undulations, 'cu', and radial, delicate striae, 's'. A zone of hackles, 'h', resides on the fringe, 'f', which is separated from the mirror plane by a mirror boundary, 'mb'. Note that the fringe forms an angular relationship with the mirror plane (from Bahat, Rabinovitch & Frid, 2005, fig. 2.30a). (e) A profile of the joint shown in (d), maintaining the same inscriptions, and showing the angle φ which the fringe forms with the mirror plane.

https://doi.org/10.1017/S0016756808004974 Published online by Cambridge University Press

type' the breakdown is 'continuous', initiating at various locations on the parent joint, and there is no clear boundary that separates the fringe from the parent joint (Fig. 3b). In the 'discontinuous breakdown type', new plumes start to form on the en échelon cracks (e.g. Woodworth, 1896; Hodgson, 1961; Bankwitz, 1966; Bahat, 1997), suggesting separate fracture events. In the 'continuous breakdown type', on the other hand, the plume propagates continuously from the parent joint to the en échelons (Bahat, 1997), implying a probable single fracture event. The literature records 'transitional' variations between the 'continuous breakdown type' and 'discontinuous breakdown type' end-members, which show plumes that cross unclear, irregular or discontinuous ('zig zag') boundaries, when continuing to propagate on the en échelon cracks that reside on fringes (e.g. Bankwitz, 1965; Roberts, 1995). Examples of the 'continuous breakdown type' and 'transitional' variations are shown by Simón, Arlegui & Pocoví (2006, figs 5b and 3a, b, respectively). In considering these geometric variations in the context of defining the mirror boundaries, it appears that only the 'discontinuous breakdown type' provides clear boundaries. They are the 'shoulders' that separate the parent joints and fringes in the classic work by Hodgson (1961).

Simón, Arlegui & Pocoví (2006) made the important distinction between 'rectangular' and 'circular' joints. The 'rectangular' joints are decorated by straight, horizontal fringes, which are controlled by the layer boundaries (Fig. 3a). The 'circular' joints are not controlled by layer boundaries and have curved fringes (Fig. 3c). As such, the fringe boundaries of the latter joints resemble (rare) curved boundaries of hackle fringes (Fig. 3d, e). Thus, curved 'discontinuous breakdown type' boundaries of en échelon fringes can be equated with mirror boundaries.

2.b. Criteria for elucidating the mirror boundaries

We now consider general criteria for elucidating 'discontinuous breakdown type' mirror boundaries on joint surfaces. At least one of the following two criteria must be identified on a joint surface for determining a mirror boundary, while the third and fourth criteria can increase the credibility of the definition.

(1) There is an abrupt morphological increase in the size of the cracks across the mirror boundary, from plumes, or delicate radial striae, to rough en échelon cracks on the fringe (Fig. 3c). The transformation of delicate radial striae to hackles on the fringe is another example of a stepwise growth beyond the mirror boundary (Fig. 3d).

There is a fundamental difference between the fractographies exhibited by Figure 3c and d, which represent 'circular' joints on the one hand, and Figure 3a, which represents 'rectangular' joints on the other. In the 'circular' joints the mirrors and fringes were not influenced by boundary effects, which enabled them to reach circular boundaries. Boundaries of 'circular' (penny-shaped) joints can be used for calculation of palaeostresses (Bahat & Rabinovitch, 1988). On the other hand, in 'rectangular' joints, the mirror boundaries are strongly influenced by the layer boundaries ('boundary effects'), such that they are forced to form parallel to them. This constraint prevents the joint from reaching circular boundaries, which would be attained when the lowest free energy conditions and equilibrium are reached. Such joints cannot be used for palaeostress calculations.

(2) A tilt fringe angle, ϕ, is formed between the imaginary continuation of the mirror plane and the fringe plane. Maximum f is seen in profile rather than in plan view, that is, looking in the direction that parallels the line of mirror boundary (Fig. 3e).

(3) Apart from size difference between plumes and fringe cracks, there are occasionally changes in the sense of stepping in the transition from the plume to the en échelon segmentation on the fringe that can be readily recognized (Bahat, 1997).

(4) The ratio of mirror plane radius to the radius of the critical flaw should be 15 ± 5 (Bahat & Rabinovitch, 1988). Straightforward estimation of this ratio is limited to exposures where the two fractographic parameters are accessible for measurements.

3. Three distinct associations of plume morphologies

As much as detailed studies of individual plumes have proved to be rewarding (e.g. Syme-Gash, 1971), more intriguing are perhaps the investigations of multi-plume associations that occur on different joint sets which crop out at close vicinities in layered rocks, or of the same sets exposed next to each other in granites. Here we make distinctions among three 'cases' of plume morphologies on joint surfaces and their fracture mechanic implications:

Case 1. Superposing plume morphologies from 'early joints' in layered rocks (those that formed before uplift), on a semi-quantitative v versus K_I curve.

Case 2. Superposing plume morphologies from both 'early joints', and 'late joints' in layered rocks (those that formed by uplift), on a semi-quantitative v versus K_I curve.

Case 3. Plotting plume morphologies from joints cutting granites on a semi-quantitative v versus K_I curve.

3.a. Case 1

3.a.1. The S- and C-type plumes from the Appalachian Plateau

We consider the particular fractographies that were distinguished on cross fold joint sets (normal and sub-normal to the fold axis) cutting the clastic sediments of the Devonian Catskill Delta in the Appalachian Plateau from New York and Pennsylvania (Bahat & Engelder, 1984). These authors found the S-type plumes (Fig. 1a) on the set oriented 345° (NNW-striking) and the C-type plumes (Fig. 1b, c) on the set oriented 335°

https://doi.org/10.1017/S0016756808004974 Published online by Cambridge University Press

(NNW-striking). As opposed to scale effects that concern the application of rock strength derived in the laboratory to large rock masses, the application of fracture mechanic parameters such as v versus K_I in fractography is not scale-dependent.

The C-type plumes are discontinuous, most probably indicating intermittent drastic reduction in velocity, possibly down to arrest (that took place whenever the driving force of pore pressure was exhausted), hence, it periodically vacillates between the stress corrosion limit and region II (Fig. 2), in analogy to the glass experimental results of Kerkhof (1975).

The continuity of the lengthy S-plumes (one of them is about 100 m long: Bahat, 1991, fig. 3.18) and the lack of arrest marks along them indicates that there were no stops or any significant reduction in velocity along its continuous propagation path. This implies (by following the fracture mechanic rule that the fracture stress multiplied by the square root of the fracture length equals a stress intensity constant K_I) that K_I and the associated fracture velocity are likely to increase with fracture length, possibly up to K_{Ic}. We observe, however, that the S-plumes do not end in hackles, hence the propagation of the joint never reached K_{Ic} conditions, probably due to the constraint imposed by the overburden. Thus, v and K_I are probably around region III. This argument is supported by the following experimental results. The striae induced by Michalske (1984, fig. 1) developed on a smooth fracture surface of soda-lime silica glass in water when the velocity of fracture propagation reached about 10^{-2} m/s at around $K_I = 0.7$–0.8 MPa $m^{1/2}$, which was above the mid-range between the stress corrosion limit, $K_I = 0.3$ MPa $m^{1/2}$, and the fracture toughness $K_{Ic} = 0.9 \pm 0.1$ MPa $m^{1/2}$, that is, within region III (Fig. 2).

Moreover, the characteristic different appearances of the two plume types in two distinct joint sets cutting siltstone (C-type plumes in set 335° and S-type plumes in set 345°) are in line with our kinetic explanation: they originated under different stress fields (e.g. distinct settings of principal stresses) that induced non-conjugate fractures at different times. Apparently, the inertia of a fast-moving crack (S-type plume) tends to drive it monotonously, while a slow fracture (C-type plume) responds more readily to minute changes in local stresses, and is more likely to deviate from straightness (Fig. 1b, c).

The basic argumentation for suggesting that the S-type plume propagated faster than the C-type plume was outlined by Bahat (1991, p. 234). Engelder (2004, fig. 4) showed similar relationships (replacing the S-type plume and the C-type plume, by J_1 and J_2, respectively).

3.a.2. The construction of the v versus K_I curve for the S- and C-type plumes

Bahat, Bankwitz & Bankwitz (2003) introduced a semi-quantitative v versus K_I curve correlative to fractographic patterns (Fig. 4). We adapted this approach in constructing semi-quantitative v versus K_I curves for the S-type and C-type plumes (Fig. 5). The initiating points of region I occur at K_I values between 0.073 MPa $m^{1/2}$ and 0.14 MPa $m^{1/2}$. These were calculated according to Atkinson & Meredith (1987*a*, fig. 4.7) by extrapolating the lowest two curves of the Tennessee sandstone to a velocity of 10^{-8} m/s. The Tennessee sandstone is the closest approximating rock to the siltstone and fine-grained sandstone beds in which the two plume types where found in at least four formations by Engelder (2004). Atkinson & Meredith (1987*a*) identified indications of the presence of region II, but have not made definitive observations of region III in rocks, although they are quite common in glasses and ceramics (Wachtman, 1974). Therefore, a hypothetical region III is added above region II in Figure 5, to facilitate clarifying the ranges of velocities and stress intensities under consideration. The two log v versus log K_I curves in region III end in a range of K_{Ic} values between 0.45 MPa $m^{1/2}$ and 0.79 MPa $m^{1/2}$ (Atkinson & Meredith, 1987*b*, table 11.3) in Figure 5.

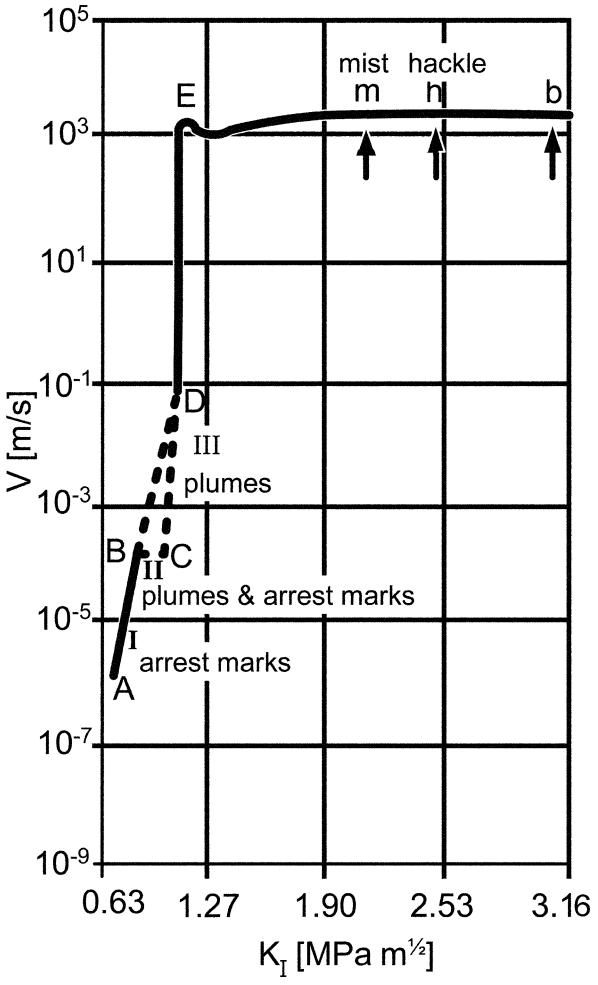

Figure 4. A semi-quantitative v versus K_I curve for joints in granite from the South Bohemian Batholith in the Czech Republic. The curve is derived from nine criteria, based on laboratory experiments and theoretical considerations, showing the approximate locations of the various fractographic elements (modified after Bahat, Bankwitz & Bankwitz, 2003).

https://doi.org/10.1017/S0016756808004974 Published online by Cambridge University Press

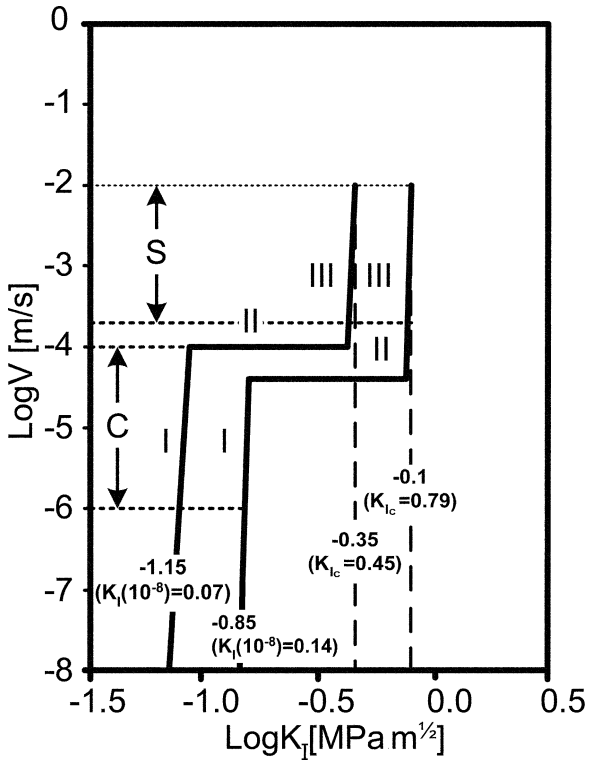

Figure 5. A semi-quantitative v versus K_I curve for the S-type and C-type plumes representing joints in the Appalachian Plateau; see calculation procedure in the text (Case 1). Plots for the two plume types vary between $K_{Ic} = 0.45$ MPa $m^{1/2}$ and $K_{Ic} = 0.79$ MPa $m^{1/2}$, based on data from Atkinson & Meredith (1987*a*).

We postulate $v(K_{Ic}) = 10^{-2}$ m/s, to be somewhat below the $v(K_{Ic})$ of granite (Fig. 4).

The sub-critical part of the log v versus log K_I curve can be estimated as follows. A well-known, semi-empirical law states that the velocity increases with K_I as (e.g. eq. 1.144 in Bahat, Rabinovitch & Frid, 2005):

$$v = aK_I^n \qquad (1)$$

where a and n (called the sub-critical crack growth indices) are constants. We use for $K_I = 0.073$ MPa $m^{1/2}$ the value of $n = 14$ and for $K_I = 0.14$ MPa $m^{1/2}$ the value of $n = 26$, according to Atkinson & Meredith (1987*b*, table 11.6) for the Tennessee sandstone in the corresponding different conditions. Constant a is not required for drawing the v and K_I curve in region I, since we know the initial point of region I, and the n values determine the slopes of the curves.

Both C and S plumes propagated in sub-critical ranges (Table 1), such that the ranges of K_I were limited by the two curves shown in Figure 5. The periodic smooth fracture of the C plume that follows the rhythmic increase in barb intensity (Fig. 1c) represents conditions between the lower limits of region I, possibly at about 10^{-6} m/s fracture velocity, in the smooth zone, and about 10^{-4} m/s in the zone that shows the radial short barbs. The latter value is somewhat above 4×10^{-5} m/s, the approximate upper value of arrest marks in plate glass (Kerkhof, 1975), and is assumed to correspond to the lower ranges of plume velocities. We suggest that region II for the S and C plumes varies between the latter two values, 10^{-4} m/s and 4×10^{-5} m/s, S closer to the upper value and C nearer to the lower one. Savalli & Engelder (2005, fig. 13B) suggested that region II for these rocks falls close to 10^{-2} m/s. The S plume mostly propagated at the high velocities of striae (Michalske, 1984), between around 2×10^{-4} m/s and close to 10^{-2} m/s (Tables 1, 2).

3.b. Case 2

3.b.1. The 'Lower Eocene plume' and 'Middle Eocene plume' in the Beer Sheva syncline

The Beer Sheva syncline is an asymmetrical fault-fold basin within the Syrian Arc (Krenkel, 1924), a sigmoid fold system that stretches from Syria in the north, through Israel to Egypt in the south. This study concerns the Mor Formation and the Horsha Formation, from the Lower and Middle Eocene, respectively, each of them about 100 m thick. The Mor Formation consists of chalk layers (40 to 90 cm thick) alternating with beds of chert nodules, up to 10 cm thick. The cross-fold single layer joints oriented 328° form the dominant set, arrested at the boundaries of the chalk layers with chert beds. Chert does not occur in the overlying Horsha Formation, which consists only of chalk layers of various thicknesses. The single layer

Table 1. Plume morphologies on joint surfaces with their fracture mechanic implications

Province number	Plume	Relation to K_{IC}	Range on the extended Wiederhorn Curve	Fracture province
(1)	Rhythmic plume C*	Sub-critical $<K_{IC}$	From stress corrosion limit to region II	Appalachian Plateau, Devonian, siltstone
	Curving plume C*	Sub-critical $<K_{IC}$	From region I to region II,	Appalachian Plateau, Devonian, siltstone
	Straight plume S*	Sub-critical $<K_{IC}$	In region III	Appalachian Plateau, Devonian, siltstone interbedded with shales
(2a)	Coarse straight plume**, in association with arrest marks	Sub-critical $<K_{IC}$	In region I	Lower Eocene chalks Burial, single-layer
(2b)	Delicate straight plume**, no association with arrest marks	Sub-critical $<K_{IC}$	Up to region III	Middle Eocene chalks Uplift, single-layer
(3)	Ten joints from Borsov quarry***	Both, sub- and post-critical $<K_{IC}>$	From region I to the hackle zone	South Bohemian Batholith, in the Czech Republic

Source: *Bahat & Engelder, 1984; **Bahat, 1987; ***Bahat, Bankwitz & Bankwitz, 2003.

https://doi.org/10.1017/S0016756808004974 Published online by Cambridge University Press

Table 2. Conditions of fracture velocities for assumed ranges of stress intensities* for joints cutting siltstone and chalk

Province number	Plume	Range of initial K_I (MPa $m^{1/2}$)	Range of K_{IC} (MPa $m^{1/2}$)	Range of fracture velocities (m/s)
(1)	Rhythmic plume C	0.073–0.14	0.45–0.79	10^{-6} –10^{-4}
	Straight plume S (Devonian siltstone)	0.073–0.14	0.45–0.79	2×10^{-4} –10^{-2}
(2a)	Coarse straight plume, in association with arrest marks (Lower Eocene chalk)	0.03–0.065	0.17	10^{-6}–4×10^{-5}
(2b)	Delicate straight plume, no association with arrest marks (Middle Eocene chalk)	0.03–0.065	0.17	5×10^{-3}–10^{-4}

*See text for sources and criteria leading to stress intensity assumptions.
See description of fracture provinces in Table 1.

joints of the Horsha Formation vary considerably in orientation (Bahat, 1987).

Practically all the joints that reveal their fractographies in the Beer Sheva fracture province are decorated by plumes. Case 2 relates to two plume types in this syncline (Bahat, 1987, 1999). The plumes that decorate single-layer burial joints, which cut the Lower Eocene chalks, are coarse and closely associated with abundant rough arrest marks (e.g. shown on the book cover of Bahat, 1991). On the other hand, the plumes that mark single-layer uplift joints in the Middle Eocene chalks are delicate and are mostly not associated with arrest marks (Fig. 3b).

These distinct fractographies most likely recorded propagation at different fracture velocities: slower in the Lower Eocene chalks, and faster in the Middle Eocene chalks. The Lower Eocene single layer joints developed in the burial stage by extension (horizontal $ó_3$ positive). The coarse plumes and rough arrest marks appeared when fracturing propagated, while being permanently covered by additional sediments under increasing overburden stresses. On the other hand, previous studies have shown that the Middle Eocene single layer joints had been formed by uplift, under growing tensile conditions when upper sediments were being removed by erosion (Bahat, 1999). Hence, fracturing initiated near to the surface, and as elevation progressed, compensation by erosion gradually exposed the rock from levels of greater depths to this maximal tension (Bahat, 1991, p. 296), that is, these joints grew in response to a stress gradient in which the horizontal least principal stress ($ó_3$ negative) migrated downward as the erosion progressed.

Correspondingly, it is likely that fracture velocity was greater when propagating close to the ground surface under tensile conditions, compared to the velocity under conditions of increasing compression with depth. Although faster propagating than the Lower Eocene joints, no hackles have been observed on any Middle Eocene joint, implying conditions of K_I below K_{Ic}.

Thus, whereas the coarse plumes from the Lower Eocene, which are commonly associated with arrest marks, correspond to a certain fracture velocity range, signifying the Lower Eocene plumes, the delicate plumes from the Middle Eocene that are not associated with arrest marks correspond to another range, signifying the Middle Eocene plumes (Fig. 6).

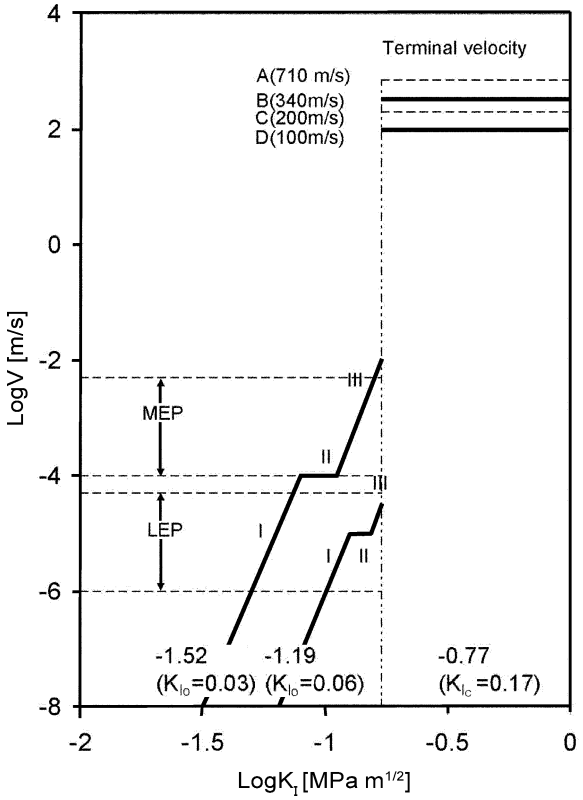

Figure 6. A semi-quantitative v versus K_I curve for joints in chalks from the Beer Sheva syncline; see calculation procedure in the text (Case 2). The frames LEP (for the coarse plume from the Lower Eocene chalks) and MEP (for the delicate plume from the Middle Eocene chalks), mark the fracture velocity limits of the two joints, below and above region II, respectively. Range of terminal velocities, between A and B for dry chalk and between C and D for wet chalk. K_{Io} is the stress intensity at the stress corrosion limit.

3.b.2. The construction of the v versus K_I curve for the 'Lower Eocene plume' and the 'Middle Eocene plume' in the Beer Sheva syncline

The construction of the logarithmic v versus K_I curve for joints in chalks from the Beer Sheva syncline (Fig. 6) is based on data from various outcrops. The value $K_{Ic} \sim 0.17$ MPa $m^{1/2}$ was borrowed from the data on chalk by Dibb, Hughes & Poole (1983). The range

https://doi.org/10.1017/S0016756808004974 Published online by Cambridge University Press

of the initiating points of region I used in Figure 6 was between K_I ($v = 10^{-8}$) = 0.03 MPa $m^{1/2}$ and 0.065 MPa $m^{1/2}$. It was calculated according to Atkinson & Meredith (1987*a*, fig. 4.14) by extrapolating the lowest curves of the calcite rocks to low velocities. This yielded the range of K_I/K_{Ic} to be from 0.16 to 0.38, respectively. Thus, K_I ($v = 10^{-8}$) varied from $0.16 \times K_{Ic} = 0.16 \times 0.17 \sim 0.03$, up to $0.38 \times 0.17 = 0.065$ MPa $m^{1/2}$.

The two curves were created by joining the respective points of K_I ($v = 10^{-8}$) to the K_{Ic} ones by following the procedure outlined for case 1 in constructing the sub-critical part of the log v versus log K_I. According to Atkinson & Meredith (1987*a*, table 11.6), n for wet marble is ~ 9. Chalks may have different stiffnesses, depending on their particle and water constitution as well as their lithological histories (Mimran, 1977, 1985). The chalks under consideration here are rather indurated (Bahat, 1987), that is, relatively stiff. Since no additional constants from carbonate rocks are to be found, we used the closest available one, from wet marble. The crack velocity at K_{Ic}, v_C is postulated to be between 10^{-4} m/sec and 10^{-2} m/s, crossing $K_{Ic} = 0.17$ MPa $m^{1/2}$ at two locations.

Both plumes propagated in sub-critical ranges, limited by the two curves shown in Figure 6. The 'Lower Eocene plume' is estimated to have propagated between about 10^{-6} m/s and 4×10^{-5} m/s, close to the range of rib markings in plate glass and somewhat below it (Kerkhof, 1975), mainly below region II. The 'Middle Eocene plume' is estimated to have propagated between about 5×10^{-3} m/s, a little below the fracture velocity of striae in soda-lime glass under water (Michalske, 1984) and about 10^{-4} m/s, mainly above region II. This velocity range was lower than for the S plumes that showed a high degree of continuity (Fig. 1a; Bahat, 1991, fig. 3.18). The curves of the 'Lower Eocene plume' and the 'Middle Eocene plume' are constructed such that region II has the 10^{-4} m/s and 4×10^{-5} m/s values, respectively (Fig. 6), as in Figure 5, although it could change somewhat, because this region is controlled by the rate of reactant (water solution) transport to the crack tip (Wiederhorn, 1967), conditions unknown to us in these two rocks.

The range of terminal velocities between A and B for dry chalk is adapted from T. Levi (unpub. M.Sc. thesis, Ben Gurion Univ. Negev, 2003) and Bahat, Rabinovitch & Frid (2005, p. 466), and taken to be between 710 m/s and 340 m/s. However, the range of terminal velocities between C and D for wet chalk is assumed to be more realistic, between 200 m/s and 100 m/s. Crack velocities are generally proportional to sound velocities in the medium. The latter are proportional to $(G/r)^{1/2}$, where G is the shear modulus and r is the density. According to G. Hayati (unpub. Ph.D. thesis, Israel Inst. Technology, 1975, fig. 4.34), the elastic moduli dependence on wetness for chalks having densities around 1400 kg/m^3 (similar to the density of the present chalk), is G(dry)/G(wet) ~ 9. Assuming a density increase of ~ 1.3 when wet (assuming minimal change in volume as water fills in the pores, when porosity is about 0.3), the decrease of velocity is about $(9 \times 1.3)^{1/2} \sim 3.4$, yielding 710/3.4 and 340/3.4 as the velocity limits in wet chalks, that is, the maximum and minimum terminal velocities, C and D, respectively, in Figure 6.

3.c. Case 3

Case 3 relates to a study of ten distinct fractographies on ten adjacent joints from the same set at the Borsov granite quarry in the South Bohemian Batholith (also termed South Bohemian Pluton) from the Czech Republic (Bahat, Bankwitz & Bankwitz, 2003; Bankwitz *et al.* 2004), which belongs to the internal zone of the Variscan belt of Europe. The country rock consists predominantly of kyanite–sillimanite-bearing gneisses and schists of Late Proterozoic to Early Palaeozoic age metamorphism at 320–330 Ma (Petrakakis, 1997; Gerdes *et al.* 2003: Tropper *et al.* 2006).

Compared to the uniformity of the fractographic features on each joint set from the Beer Sheva sedimentary syncline, and to a large extent, also on the two sets from the Appalachian Plateau, there is a great fractographic variability in the Borsov granite quarry. Whereas in the two sedimentary provinces the plume features prevail, with a minor appearance of arrest marks, all confined to the sub-critical side of the v versus K_I diagram (Fig. 2), the fractography from the Borsov granite quarry consists essentially of almost all the known, conventional brittle fracture elements (Bahat, Bankwitz & Bankwitz, 2003). A semi-quantitative curve of v versus K_I was constructed for the joints at Borsov, showing that these joints were distributed between very low and very high values of v and K_I (along most of the curve shown in Fig. 4; see also Table 1). This wide spread of values was interpreted as an indication that the joints had been formed by high pore pressures in the cooling granites, which locally varied considerably at the locations of individual joints.

4. Discussion

4.a. The absence of hackles in the investigated sedimentary rock layers

Cases 1 and 2 here received treatments as close to quantitative as possible, noting some of the existing limitations of the method (Bahat, Bankwitz & Bankwitz, 2003). In these relatively thin layers (up to about 50 cm in the siltstones of the Appalachian Plateau, and about 90 cm thickness in the chalks of the Beer Sheva syncline), plane stress conditions gradually increase from the middle of the rock layers towards their boundaries (Bahat, 1991, pp. 26, 246). Under these conditions, K_{Ic} values reach their maximum (Broek, 1982), compared to low K_{Ic} values in thick layers where plane strain conditions prevail. Accordingly, the difficulty of attaining fracture toughness (K_{Ic}) conditions in thin sedimentary layers is why hackle

https://doi.org/10.1017/S0016756808004974 Published online by Cambridge University Press

formation in these rocks is likely to be minimal. In granites, on the other hand, hackles are more likely to occur, where plane strain conditions are more common.

4.b. The multiple geological influences on plume morphologies that must be considered in conjunction with the fracture mechanic analysis

We explained above our reasons for suggesting why in case 1 the coarser plumes were faster than the smoother ones, and in case 2 the plumes with the more delicate morphologies were faster than the plumes with the coarser morphologies. The implication is that when correlating K_I and v conditions to plume characteristics in different fracture provinces, various geological parameters have to be taken into account, because these two fracture mechanic properties represent the sum of mechanical parameters that stem from the overall, local geological conditions, some of which influence the jointing process. We consider below several such parameters, including: (1) layer thickness, (2) joint genetics, (3) pore pressure, (4) supporting fractographic observations, (5) lithology and (6) interdependent relationships.

(1) It has been remarked that plumes like the S type are correlative with the reduction of layer thickness (Roberts, 1961; Syme-Gash, 1971). This relationship can be linked to the 'fracture slanting' model, stemming from studies by Hertzberg (1976), Broek (1982) and others. This is the reason why there is an increase in the occurrence of coarse S-type plumes in thinner layers. Apparently, slant cracks in thinner plates propagate more rapidly than those in thicker ones (Bank-Sills & Schur, 1989).

(2) As mentioned above, while single layer jointing of the Lower Eocene chalks was of the burial genetic type, jointing of the Middle Eocene chalks took place during uplift(s). A somewhat similar correlation is seen in the Appalachian Plateau. Arrest marks of the C type occurred on slowly propagating joints (Fig. 1c) from the burial stage under increasing overburden stresses, while the rock has been constantly covered by additional sediments. On the other hand, arrest marks were absent from the S-type joints that formed during the syntectonic stage (Bahat, Rabinovitch & Frid, 2005, p. 205), when tectonic forces partly overcame the retarding influence of the overburden on fracture propagation.

    Thus, there is a correlation between the fracture conditions characteristic to the various genetic jointing stages, the joint velocities and the corresponding induced fractographies. In the two investigated sedimentary fracture provinces, jointing in the burial stage was slow because it was constrained by heavy overburden, which resulted in fractographies enriched in arrest marks. During the syntectonic and uplift stages, overburden pressures were neutralized by counter-stresses that induced faster fracturing as recorded by plumes, mostly without arrest marks.

(3) The discovery of the C plumes on joint surfaces (Fig. 1c) suggested to Bahat & Engelder (1984) that the mechanism proposed by Secor (1965) for fracture propagation at depth is applicable in interpreting certain jointing processes. Secor's model fits quite well the formation mechanism of burial joints which are primarily driven by pore pressure, but it is doubtful whether this mechanism can also explain the growth of uplift joints, which result from remote tension, quite likely caused by bending (Price, 1974; Bahat & Rabinovitch, 1988). The role of pore pressure in forming syntectonic joints depends on the overall stress conditions imposed by opposing remote tectonic stresses and local pore pressures, and may change from case to case. It appears that the formation of the S-type plumes, which do not reveal periodicity analogous to that exhibited by the rhythmic C-type plume, was less affected by pore fluid pressures than the latter plume type, and perhaps not affected at all.

(4) Supporting evidence for the interpretation suggested above comes from several experimental observations, which have shown that arrest marks precede striae (and plumes) as fracture propagation proceeds (e.g. Bahat, 1991, pp. 136, 235). Therefore, the presence or absence of arrest marks is a diagnostic criterion in establishing the velocity ranges of plume propagation.

(5) Different lithologies would supply different amounts and pressures of pore driving forces for jointing.

(6) It appears that there are some interdependent relationships between the influences of the layer thickness, joint genetics and pore pressure on the plume morphology. The increase of overburden pressure during the burial stage imposes a constraint on the jointing velocity. This is overcome by periodic bursts of pore pressure, as often recorded on rhythmic plumes (Fig. 1c).

Thus, given an increase in layer thickness, a lithology that would supply proper amounts of fluids and strong overburden pressures would tend to create rhythmic short C-type plumes and arrest marks. On the other hand, decreasing overburden pressures and reduced effectiveness of pore pressures would favour the formation of lengthy, coarse S-type plumes and absence of arrest marks. When all other conditions are the same, thicker layers would be marked by more delicate plumes, whereas thinner layers would be decorated by coarser plumes.

https://doi.org/10.1017/S0016756808004974 Published online by Cambridge University Press

4.c. Isotropic and anisotropic conditions

There is a need to distinguish between two fracture cases: (a) an idealistic, isotropic one (remote from boundary conditions), and (b) a fracture influenced by boundary conditions, rendering it anisotropic. Plumes will not form under conditions of no resistance to pure tensile fracture, often seen on a dynamically fractured glass under idealistic, isotropic conditions. However, dynamic fracture in glass, or glass ceramic (which is dominated by the glassy phase), when propagating between neighbouring boundaries, induces a series of curving striae that form a plume (Bahat *et al.* 2002). In fact, these striae are even split (microscopically) into secondary ones, imitating plumes (Goldbaum *et al.* 2003), a process characteristic of plumes often seen on joint surfaces. In addition, on the joint surface of a given rock, coarseness of plumes generally changes inversely with fracture velocity. Delicate plumes are created when some resistance is translated to local mode III shear, which retards the propagation of joints, due to the 'mode III crack closure effect' (Tshegg, 1983). When the latter parameter becomes more pronounced, coarse plumes are developed.

5. Limitations and open questions

There are limitations in our comprehension of the observations. Particularly, the calculations lead us to estimate (rather than determine) our geological results, due to certain restrictions, as itemized below.

(1) We investigate fracture processes only at their post-mortem stage, measure strain results via their fractographic record, and translate it to K_I and v parameters. By doing this, we probably introduce errors into our calculations.

(2) At the base of our calculations we made the following assumptions: (a) The shape of the v versus K_I diagram has a universal shape, at least for the sub-critical regime. (b) We have used results of materials (rocks) similar to the ones treated because of lack of experimental results for the actual ones. This may be important, especially for the exponent value n. (c) Velocity values at K_{Ic} are hard to estimate experimentally, and we have therefore used a wide range of values.

    Consequently, the final estimates for the velocities and K_I values of the S and C plumes, as well as for the Lower Eocene plume and Middle Eocene plume cases cannot be considered to be precise. However, the approximate fracture mechanic conditions do clearly emerge.

(3) Although, generally considered to indicate slow fracture velocities (e.g. Kulander, Barton & Dean, 1979; Müller & Dahm, 2000), en échelon segmentation may occasionally indicate high velocities (Cramer, Wanner & Gumbsch, 2000). This is because the en échelon breakdown is dependent on the ratio of mode III/mode I (Sommer, 1969), and when this ratio decreases, rare, rapid fracturing may occur. In this connection, we still do not know how to identify the critical conditions that would result in en échelon segmentation or in hackles. For instance, the case shown by Bahat, Grossenbacher & Karasaki (1999), and Figure 3c herein, needs to be further investigated along this line.

(4) In another example, Peter Bankwitz (pers. comm.) observed different relationships of K_{III}/K_I and plume morphology versus layer thickness (in non-sedimentary rocks) from the one mentioned in Section 4.b. This intriguing difference needs to be examined.

(5) We still do not know how to identify the mirror boundaries for fringes of the 'continuous breakdown type' and 'transitional' styles. Perhaps some guidance may come from distorted fractographies of certain ceramics and single crystals, which often have irregular or discontinuous ('zig zag' or 'tongue') boundaries (e.g. Rice, 1974).

6. Conclusions

This paper focuses on three new subjects: (1) the mirror plane and criteria for elucidating the mirror boundaries, (2) a new method of calculating K_I and v in sedimentary rocks, and estimating the fracture velocities of four joints in two fracture provinces, and (3) arguing that the treatment of the fracture mechanics of jointing in sedimentary rocks must be carried out in conjunction with the possible variability of some six geological parameters.

A key criterion in characterizing the mirror plane is identifying the mirror boundary that separates the mirror plane and the fringe. There is a clear distinction between two en échelon segmentation types in the fringe, the 'discontinuous breakdown type', and the 'continuous breakdown type'. The present study applies only to the discontinuous breakdown type.

Four criteria for elucidating mirror boundaries on joints may be useful: (1) morphological, (2) angular, (3) sense of stepping changes across mirror boundaries and (4) the ratio of mirror plane radius/the radius of the critical flaw, which should be around 15.

There is a correlation between the fracture conditions characteristic of the various genetic jointing groups, the joint fracture velocities and the corresponding induced fractographies. Often slow plumes are relatively short, show periodicity and typically exhibit superposition of arrest marks. On the other hand, faster plumes are longer, and show no superposition of arrest marks.

The tensile stress intensity, K_I, and the velocity of joint propagation, v, are two basic fracture mechanic properties that represent the sum of mechanical parameters that stem from the overall, local geological conditions, some of which influence the jointing process. Therefore, when correlating K_I and v conditions to plume characteristics in different fracture

https://doi.org/10.1017/S0016756808004974 Published online by Cambridge University Press

provinces, various geological influential parameters have to be taken into account: (1) layer thickness, (2) joint genetics, (3) remote and local stresses, (4) pore pressure, (5) different lithologies and (6) interdependent relationships between the influences of various parameters.

The difficulty in reaching fracture toughness (K_{Ic}) conditions in thin sedimentary layers where plane stress conditions prevail minimizes the likelihood of hackle formation in them. This is an important reason why hackles are almost unknown in these rocks. In granites, on the other hand, hackles are more likely to occur, where plane strain conditions are more common. The results show that the joints considered in this study from the Appalachian Plateau, USA, and the Syrian Arc in Israel never reached the K_{Ic} conditions.

Acknowledgements. We are grateful for the most useful comments made by Peter Bankwitz and J. L. Simón on an earlier version of this manuscript. Jiří Žák, an unknown referee and the editor helped to improve the paper significantly. Yoav Borenstein and Or Bialik provided technical help. This study was supported by the Earth Sciences Administration, the Ministry of Energy and Infrastructure.

References

ATKINSON, B. K. & MEREDITH, P. G. 1987*a*. The theory of subcritical crack growth with applications to the minerals and rocks. In *Fracture mechanics of rock* (ed. B. K. Atkinson), pp. 111–66. London: Academic Press.

ATKINSON, B. K. & MEREDITH, P. G. 1987*b*. Experimental fracture mechanics data for rocks and minerals. In *Fracture mechanics of rock* (ed. B. K. Atkinson), pp. 477–525. London: Academic Press.

BAHAT, D. 1979. Theoretical considerations on mechanical parameters of joint surfaces based on studies on ceramics. *Geological Magazine* **11**, 81–92.

BAHAT, D. 1987. Correlation between styles of fracture markings and orientation of cross fold joints. *Tectonophysics* **136**, 323–333.

BAHAT, D. 1991. *Tectonofractography*. Heidelberg: Springer-Verlag, 354 pp.

BAHAT, D. 1997. Mechanisms of dilatant en échelon crack formation in jointed layered chalks. *Journal of Structural Geology* **19**, 1375–92.

BAHAT, D. 1999. Single-layer burial joints versus single-layer uplift joints in Eocene chalk from the Beer-Sheva syncline in Israel. *Journal of Structural Geology* **21**, 293–303.

BAHAT, D., BANKWITZ, P. & BANKWITZ, E. 2003. Pre-uplift joints in granites: Evidence for subcritical and post-critical fracture growth. *Bulletin American Geological Society of America* **115**, 148–65.

BAHAT, D. & ENGELDER, T. 1984. Surface morphology on cross-fold joints of the Appalachian Plateau, New York and Pennsylvania. *Tectonophysics* **104**, 299–313.

BAHAT, D., FRID, V., RABINOVITCH, A. & PALCHIK, V. 2002. Exploration via electromagnetic radiation and fractographic methods of fracture properties induced by compression in glass-ceramic. *International Journal of Fracture* **116**, 179–94.

BAHAT, D., GROSSENBACHER, K. & KARASAKI, K. 1999. Mechanism of exfoliation joint formation in granitic rocks at Yosemite National Park. *Journal of Structural Geology* **21**, 85–96.

BAHAT, D. & RABINOVITCH, A. 1988. Paleostress determination in a rock by a fractographic method. *Journal of Structural Geology* **10**, 193–9.

BAHAT, D., RABINOVITCH, A. & FRID, V. 2005. *Tensile fracturing in rocks: tectonofractography and electromagnetic radiation methods*. Heidelberg: Springer, 569 pp.

BANK-SILLS, L. & SCHUR, D. 1989. On the influence of crack plane orientation in fatigue crack propagation and catastrophic failure. *American Society for Testing and Materials, Standard Technical Publication* **1020**, 497–513.

BANKWITZ, P. 1965. Über Klufte I. Beobachtungen im Thüringischen Schiefergebirge. *Geologie* **14**, 241–53.

BANKWITZ, P. 1966. Über Klüfte II. Die Bildung der Kluftoberfläche und eine Systematik ihrer Strukturen. *Geologie* **15**, 896–941.

BANKWITZ, P., BANKWITZ, E., THOMAS, R., WEMMER, K. & KÄMPF, H. 2004. Age and depth evidence for preexhumation joints in granite plutons: Fracturing during the early cooling stage of felsic rock. In *The initiation, propagation and arrest of joints and other fractures* (eds J. W. Cosgrove & T. Engelder), pp. 25–47. Geological Society of London, Special Publication no. 231.

BROEK, D. 1982. *Elementary engineering fracture mechanics*. Boston: Martinus Nijhoff Publishers, 469 pp.

CRAMER, T., WANNER, A. & GUMBSCH, P. 2000. Energy dissipation and path instabilities in dynamic fracture of silicon single crystals. *Physical Review Letters* **85**, 788–91.

DIBB, T. E., HUGHES, D. W. & POOLE, A. B. 1983. The identification of critical factors affecting rock durability in marine environments. *The Quaternary Journal of Engineering* **16**, 149–61.

ENGELDER, E. 2004. Tectonic implications drawn from differences in the surface morphology on two joint sets in the Appalachian Valley and Ridge, Virginia. *Geology* **32**, 413–16.

EVANS, A. G. 1974. Role of inclusions in the fracture of ceramic materials. *Journal of Materials Science* **9**, 1145–52.

GERDES, A., FRIEDL, G., PARRISH, R. R. & FINGER, F. 2003. High-resolution geochronology of Variscan granite emplacement – the South Bohemian Batholith. *Journal of the Czech Geological Society* **48**(1–2), 53–4.

GOLDBAUM, J., FRID, V., BAHAT, D. & RABINOVITCH, A. 2003. An analysis of complex electromagnetic radiation signals induced by fracture. *Measurement Science and Technology* **14**, 1839–44.

HERTZBERG, R. W. 1976. *Deformation and fracture mechanics of engineering materials*. New York: John Wiley & Sons Ltd., 605 pp.

HODGSON, R. A. 1961. Classification of structures on joint surfaces. *American Journal of Science* **259**, 493–502.

HULL, D. 1999. *Fractography: Observing, measuring, and interpreting fracture surface topology*. Cambridge: Cambridge University Press, 366 pp.

KERKHOF, F. 1975. Bruchmechanische Analyse von Schadensfällen an Gläsern. *Glastechnische Berichte* **48**, 112–24.

KRENKEL, E. 1924. Der Syrische Bogen. *Centralbatt für Mineralogie, Geologie und Palaeontologie* **9**, 274–81, 10301–13.

KULANDER, B. R., BARTON, C. C. & DEAN, S. C. 1979. The application of fractography to core and outcrop fracture investigations. *Report to U.S.D.O.E. Morgantown Energy Technology Center, METC SP* **79/3**.

LACAZETTE, A. & ENGELDER, T. 1992. Fluid-driven cyclic propagation of a joint in the Ithaca siltstone, Appalachian basin, New York. In *Fault Mechanics and transport properties of rocks* (eds B. Evans & T. Wong), pp. 297–324. London: Academic Press.

MICHALSKE, T. A. 1984. Fractography of slow fracture in glass. In *Fractography of ceramic and metal failures* (eds J. J. Mecholsky & S. R. Powell), pp. 121–36. ASTM STP 827, Philadelphia.

MIMRAN, Y. 1977. Chalk deformation and large-scale migration of calcium carbonate. *Sedimentology* **24**, 333–60.

MIMRAN, Y. 1985. Tectonically controlled freshwater carbonate cementation in Chalk. In *Carbonate Cements* (eds N. Schneidermann & P. M. Harris), pp. 371–9. SEPM, Special Publication no. 36.

MÜLLER, G. & DAHM, T. 2000. Fracture morphology of tensile cracks and rupture velocity. *Journal of Geophysical Research* **105**, 723–38.

PETRAKAKIS, K. 1997. Evolution of Moldanubian rocks in Austria: review and synthesis. *Journal of Metamorphic Geology* **15**, 203–22.

PRICE, N. J. 1974. The development of stress systems and fracture patterns in undeformed sediments. In *Proceedings Third Congress of the International Society for Rock Mechanics, Denver, CO*, pp. 487–98. *Advances in Rock Mechanics* **1**.

RABINOVITCH, A. & BAHAT, D. 1979. Catastrophe theory: A technique for crack propagation analysis. *Journal of Applied Physics* **50**, 321–34.

RICE, R. W. 1974. Fracture topography of ceramics. In *Surfaces and interfaces of glass and ceramics* (eds V. D. Frechette, W. C. La Course & V. L. Burdick), pp. 439–72. New York: Plenum Publishing Corporation.

ROBERTS, J. C. 1961. Feather-fracture and the mechanics of rock jointing. *American Journal of Science* **259**, 481–92.

ROBERTS, J. C. 1995. Fracture surface markings in Liassic limestone at Lavernock Point, South Wales. In *Fractography: Fracture topography as a tool in fracture mechanics and stress analysis* (ed. M. S. Ameen), pp. 175–86. Geological Society of London, Special Publication no. 92.

SAVALLI, L. & ENGELDER, T. 2005. Mechanism controlling rupture shape during subcritical growth of joints in layered rocks. *Bulletin Geological Society of America* **117**, 436–49.

SECOR, D. T. JR. 1965. Role of fluid pressure in jointing. *American Journal of Science* **263**, 633–46.

SIMÓN, J. L., ARLEGUI, L. E. & POCOVÍ, A. 2006. Fringe cracks and plumose structures in layered rocks: stepping senses and their implications for palaeostress interpretation. *Journal of Structural Geology* **28**, 1103–13.

SOMMER, E. 1969. Formation of fracture "lances" in glass. *Engineering Fracture Mechanics* **1**, 539–46.

SYME-GASH, P. J. 1971. Surface features relating to brittle fracture. *Tectonophysics* **12**, 349–91.

TROPPER, P., DEIBL, I., FINGER, F. & KAINDL, R. 2006. P–T–t evolution of spinel–cordierite–garnet gneisses from the Sauwald Zone (Southern Bohemian Massif, Upper Austria): is there evidence for two independent late-Variscan low-P/high-T events in the Moldanubian Unit? *International Journal of Earth Sciences* **95**, 1019–37.

TSCHEGG, E. K. 1983. Mode 3 and mode 1 fatigue crack propagation behavior under torsional loading. *Journal of Materials Science* **18**, 1604–14.

WACHTMAN, J. B. JR. 1974. Highlights of progress in the science of fracture of ceramics and glass. *Journal of American Ceramics Society* **57**, 509–18.

WIEDERHORN, S. M. 1967. Influence of water vapor on crack propagation in soda-lime glass. *Journal of American Ceramics Society* **50**, 407–14.

WIEDERHORN, S. M. & BOLZ, L. H. 1970. Stress corrosion and static fatigue of glass. *Journal of American Ceramic Society* **53**, 543–8.

WOODWORTH, J. B. 1896. On the fracture system of joints, with remarks on certain great fractures. *Proceedings of the Boston Society of Natural History* **27**, 63–184.